

# On the photoproduction of jets at HERA

P. Aurenche, J.-Ph. Guillet

*Laboratoire de Physique Théorique ENSLAPP\* – Groupe d'Annecy  
LAPP, IN2P3-CNRS, B.P. 110, F-74941 Annecy-le-Vieux Cedex, France*

M. Fontannaz

*Laboratoire de Physique Théorique et Hautes Energies<sup>†</sup>  
Université de Paris XI, bâtiment 211, F-91405 Orsay Cedex, France*

## Abstract

We discuss the inclusive jet production at HERA in the next-to-leading logarithm approximation. Theoretical uncertainties are considered in some details. We show the importance of the jet rapidity distribution to constrain the parton densities in the photon. A comparison is made with the recent H1 data.

---

\*URA 14-36 du CNRS, associée à l'Ecole Normale Supérieure de Lyon, et au Laboratoire d'Annecy-le-Vieux de Physique des Particules.

<sup>†</sup>Laboratoire associé au CNRS (URA 63).

ENSLAPP-A-484/94  
LP THE Orsay 94-80  
August 1994

Several works have recently been devoted to the study of hard processes in photon-proton scattering. The renewed interest in such reactions is due to the opening up of a new kinematical domain at HERA and the publication, for the first time, of data on large transverse momentum jets in photoproduction reactions at very high energies [1]-[3]. The importance of this process arises from the possibility of probing the hadronic structure of the photon in a way complementary to the usual studies of the deep inelastic photon structure function. In the latter case, one can reach the very small  $x$  domain of the parton densities in the photon and, in particular, directly measure the quark distributions whereas the gluon distribution is constrained by the evolution equations. On the contrary, in photoproduction reactions one directly probes the gluon density in the photon assuming the parton distributions in the proton are known from elsewhere. A quantitative study of both processes together should then lead to a precise determination of the photon structure very much in the same way as it does in purely hadronic reactions. As we shall see, the non perturbative input to the photon structure function will also be constrained by hard processes in photoproduction.

In the following we consider the next-to-leading logarithm predictions of large  $p_T$  jet production with emphasis on the interplay between processes where the photon couples directly and those where it interacts through its parton contents. Some theoretical uncertainties are analysed. We then discuss in which kinematical domain the future HERA data will be able to constrain the parton distributions. A comparison with present data from H1 is performed and we discuss in particular the role of the gluon distribution. We stress the importance of the rapidity distribution in the determination of the photon structure functions.

Several theoretical papers have already appeared on the subject [4], [5]. Contrary to previous works we stress the phenomenological relevance of jet photoproduction data and indicate what precision the data should reach and what rapidity domain should be explored to extract useful physics information.

# 1 The photon-proton cross section

We first consider the scattering of a real photon off a proton at a fixed center of mass energy  $\sqrt{s}$ . The cross section for the production of a jet of transverse momentum  $p_T$  and pseudo-rapidity  $\eta$  can be written

$$\frac{d\sigma}{d\vec{p}_T d\eta} = \frac{d\sigma^D}{d\vec{p}_T d\eta} + \frac{d\sigma^{SF}}{d\vec{p}_T d\eta} \quad (1)$$

where the first term on the right-hand side involves the "direct" coupling of the photon to the hard partonic process while the second term describes the interaction of the photon through its "structure function". In the next-to-leading logarithmic approximation these terms take the form

$$\begin{aligned} \frac{d\sigma^D}{d\vec{p}_T d\eta}(R) &= \sum_{i=q,g} \int dx_1 F_{i/p}(x_1, M) \\ &\quad \frac{\alpha_s(\mu)}{2\pi} \left( \frac{d\sigma^{i\gamma \rightarrow jet}}{d\vec{p}_T d\eta} + \frac{\alpha_s(\mu)}{2\pi} K_{i\gamma}^D(R; M, \mu) \right) \end{aligned} \quad (2)$$

and

$$\begin{aligned} \frac{d\sigma^{SF}}{d\vec{p}_T d\eta}(R) &= \sum_{i,j=q,g} \int dx_1 dx_2 F_{i/p}(x_1, M) F_{j/\gamma}(x_2, M) \\ &\quad \left( \frac{\alpha_s(\mu)}{2\pi} \right)^2 \left( \frac{d\sigma^{ij \rightarrow jet}}{d\vec{p}_T d\eta} + \frac{\alpha_s(\mu)}{2\pi} K_{ij}^{SF}(R; M, \mu) \right) \end{aligned} \quad (3)$$

which exhibit the higher order corrections to the hard processes  $K_{i\gamma}^D(R; M)$  and  $K_{ij}^{SF}(R; M, \mu)$  respectively [6]. The latter term is the same as in purely hadronic reactions and has been calculated some time ago in [7] while the former term has recently been computed and used in photon-photon collisions [8]. For consistency, the parton distributions in the proton,  $F_{i/p}(x, M)$ , and in the photon,  $F_{j/\gamma}(x, M)$ , also have to be defined beyond the leading-logarithm approximation. The parameter  $R$  specifies the jet cone size, while  $\mu$  and  $M$  are the renormalization and factorization scales respectively. The factorization decomposition eqs. (2,3), involving external photons, and has been derived in the  $\overline{MS}$  scheme [9] using the technics of [10] and [11].

Since one of the aims of this work is the determination of the parton distributions in the photon we now discuss the functions  $F_{i/\gamma}(x, M)$  in some

details. They satisfy evolution equations of type (we assume one flavor for simplicity)

$$\frac{dF_{i/\gamma}}{d\ln M^2} = k_i + P_{ij} \otimes F_{j/\gamma}, \quad (4)$$

with

$$P \otimes F_{i/\gamma} = \int_x^1 dz P\left(\frac{x}{z}\right) F_{i/\gamma}(z) \quad (5)$$

Both the Altarelli-Parisi kernels  $P_{ij}$  and the inhomogeneous terms  $k_i$  have a perturbative expansion in terms of the strong coupling constant,

$$\begin{aligned} P_{ij} &= \frac{\alpha_s(M)}{2\pi} (P_{ij}^{(0)} + \frac{\alpha_s(M)}{2\pi} P_{ij}^{(1)}) \\ k_i &= \frac{\alpha}{2\pi} (k_i^{(0)} + \frac{\alpha_s(M)}{2\pi} k_i^{(1)}) \end{aligned} \quad (6)$$

The expressions for the various terms, in the  $\overline{MS}$  scheme, can be found in [12] and in [13], [14] respectively. The general solution of eqs. (4) is written as a superposition of two terms,

$$F_{i/\gamma}(x, M) = F_{i/\gamma}^{AN}(x, M) + F_{i/\gamma}^{NP}(x, M) \quad (7)$$

where the first term on the right hand side satisfies the full inhomogeneous equation and vanishes at some initial  $M = M_0$  value whereas the "non-perturbative" term obeys the homogeneous evolution equation. It will be discussed at length below.

The parton distributions are defined with respect to some physical process which is usually taken as the deep-inelastic photon structure function  $F_2^\gamma(x, Q)$ . The relation between the structure function and the parton distributions is given by:

$$F_2^\gamma(x, Q) = F_{q/\gamma}(x, Q) \left(1 + \frac{\alpha_s(Q)}{2\pi} C_q^{(1)}(x)\right) + F_{g/\gamma}(x, Q) \frac{\alpha_s(Q)}{2\pi} C_g^{(1)}(x) + C_\gamma(x) \quad (8)$$

The Wilson coefficients  $C_i^{(1)}(x)$  have been calculated long time ago [15]. We shall always assume in the following that they are defined in the  $\overline{MS}$  scheme.

The direct term  $C_\gamma$  has also been known for some time and in the  $\overline{MS}$  scheme it takes the form

$$C_\gamma(x) = 6 \frac{\alpha}{2\pi} e_q^4 \left( (x^2 + (1-x)^2) \ln \frac{1-x}{x} + 8x(1-x) - 1 \right) \quad (9)$$

When working beyond the leading logarithm approximation we are free to choose the expression of  $C_\gamma(x)$  by modifying the factorization scheme. With the  $\overline{MS}$  choice, as in the above equation, we observe that the  $\ln(1-x)$  factor becomes very large near the boundary of phase space and then it does not appear as a correction in eq. (8) since it may become numerically larger than the leading terms  $F_{i/\gamma}$  which are enhanced by a factor  $1/\alpha_s$ . In order to keep the concept of a perturbative expansion useful, it is proposed in [14] to introduce the  $DIS_\gamma$  factorization scheme where the choice

$$C_\gamma(x)|_{DIS_\gamma} = 0 \quad (10)$$

is made. The parton distributions thus defined satisfy an evolution equation of type (4) with the inhomogeneous terms  $k_i^{(1)}$  replaced by

$$\frac{\alpha}{2\pi} k_i^{(1)}|_{DIS_\gamma} = \frac{\alpha}{2\pi} k_i^{(1)} - P_{iq}^{(0)} \otimes C_\gamma \quad (11)$$

as can be immediately derived by expressing the  $\overline{MS}$  parton distributions  $F_{i/\gamma}$  in terms of their  $DIS_\gamma$  counterparts

$$\begin{aligned} F_{q/\gamma} &= F_{q/\gamma}|_{DIS_\gamma} - C_\gamma \\ F_{g/\gamma} &= F_{g/\gamma}|_{DIS_\gamma} \end{aligned} \quad (12)$$

in eq. (4). Note that the homogeneous terms are not affected by this transformation. It is shown in [14] that, in this convention, the leading logarithmic and the beyond leading logarithmic parton distributions remain very close to each other over the all range in  $x$ .

We adopt here a different approach which also absorbs the troublesome "large"  $\ln(1-x)$  terms with the added advantages that the parton distributions we define are universal (i.e. independent of the reference process) and obey the  $\overline{MS}$  evolution equations [16], as all hadron structure functions in practical use today. Furthermore they are physically motivated by a careful analysis on how to implement the non-perturbative input. One

criticism which may be raised against the procedure in [14] is the following. At  $Q = Q_0$  the structure function  $F_2^\gamma(x, Q_0)$  is entirely given by the non-perturbative quark and gluon distributions which are identified with the quark and gluon distributions in a vector meson according to the  $VDM$  hypothesis. But there is no compelling reason to make this identification in the  $DIS_\gamma$  scheme rather than in the  $\overline{MS}$  scheme (the difference is the term  $C_\gamma$ ) or even to choose another physical process where to perform the identification with the  $VDM$  input. A careful analysis [16] shows that at  $Q = Q_0$  the relationship between the photon structure function and the  $VDM$  quark distribution should be in the  $\overline{MS}$  scheme (neglecting higher order terms)

$$\begin{aligned} F_2^\gamma(x, Q_0) &= C_\gamma(x) + F_{q/\gamma}^{NP}(x, Q_0) \\ &= C_\gamma(x) - C_0(x) + F_{q/\gamma}^{VDM}(x, Q_0) \end{aligned} \quad (13)$$

with

$$C_0(x) = 6 \frac{\alpha}{2\pi} e_q^4 \left( (x^2 + (1-x)^2 \ln(1-x) + 2x(1-x)) \right) \quad (14)$$

In words, it means that the  $VDM$  hypothesis does not apply to  $F_{i/\gamma}^{NP}$ , introduced in eq. (7), but rather to the combination  $F_{q/\gamma}^{VDM} = F_{q/\gamma}^{NP} + C_0$  which is independent of the regularization scheme. Thus, the dominant part of the direct term has to be absorbed in the non-perturbative input. The function  $C_0(x)$  arises from an analysis in the collinear approximation and it reflects the singularity structure associated to the external photon leg: it is therefore independent of the hard process in which the photon is involved. In that sense the definition of our  $VDM$  input is universal, independent of the considered observable. Away from  $Q = Q_0$ , the function  $F_{i/\gamma}^{NP}$  evolves according to the homogeneous Altarelli-Parisi equations in the  $\overline{MS}$  scheme.

Roughly speaking, it can be said that in the approach of [14] the direct term is entirely absorbed in the anomalous photon component with an appropriate modification of the evolution equation ( $DIS_\gamma$  scheme) whereas, in our approach [16], part of the direct term is absorbed in the non-perturbative input at the scale  $M_0$  and then evolves with it in the usual  $\overline{MS}$  scheme.

Throughout this work we use the parton distributions defined in [16] which are adjusted to reproduce the photon structure function [17]-[20]. They are also in good agreement with the single jet production cross section in  $\gamma\gamma$  collisions at TRISTAN energies [21], [8]. The scale  $M_0$  at which the

perturbative input vanishes is  $M_0^2 \simeq m_\rho^2 \simeq .5 \text{ GeV}^2$ . The "standard set" is obtained when the full *VDM* input is used in eq. (13) but we have the flexibility of changing the overall normalization of this component so that its effect on physical quantities can be easily analysed. The *VDM* input is related to the pion structure functions of [22].

Until now no experimental results have been presented with a fixed photon-proton energy. All data involve a convolution on the photon energy. We approximate here the H1 kinematical configuration [1] and convolute the  $\gamma p$  cross section with the Weizsäcker-Williams spectrum to construct the jet cross section in  $e p$  collisions. Taking into account the experimental tagging condition we use

$$F_{\gamma/e}(z) = \frac{\alpha}{2\pi z} \left(1 + (1-z)^2\right) \ln \frac{(1-z)Q_{max}^2}{z^2 m_e^2} \quad (15)$$

where  $m_e$  is the electron mass and the maximum virtuality of the quasi-real photon is given by  $Q_{max}^2 = .01 \text{ GeV}^2$ . The photon momentum is further restricted by the condition  $.25 < z < .7$ . Let us just mention that given the smallness of the virtuality of the incoming photon it is a good approximation to neglect it altogether [23, 8, 24].

For the following studies we use for the proton structure function the quark and gluon distributions of ref. [25]. We thus have a consistent set of parton distributions since the pion distributions, used in the definition of the *VDM* component, have been derived from an analysis of  $\pi p$  data using the parametrization of [25] for the proton.

## 2 Phenomenological studies

As is well known, all perturbatively calculated cross section suffer from scale ambiguities. We illustrate this point by plotting for Hera energy,  $\sqrt{s_{ep}} = 295 \text{ GeV}$ , the variation of the cross section, at fixed jet  $p_T$  ( $p_T = 8 \text{ GeV}/c$ ) and pseudo-rapidity ( $\eta = 0$ ). In fig. 1a) the leading logarithmic predictions, *i.e.* arbitrarily setting  $K_{i\gamma}^D = K_{ij}^{SF} = 0$ , are shown: the plot reflects the monotonous variation of the coupling  $\alpha_s(\mu)$  when the factorization scale  $M$  is fixed and the monotonous variation of the structure function with  $M$  when  $\mu$  is fixed. There is no preferred point on this plot. The picture in the next-to-leading approximation is quite different (fig. 1b)) and the 2-dimensional



surface now exhibits a saddle point referred to as the "optimal point". This is seen, more quantitatively, in fig. 1c) which shows the "equipotential" lines of the surface: in particular one observes a region of stability extending roughly between  $2.2 < \mu \text{ (GeV/c)} < 4.5$  and  $2. < M \text{ (GeV/c)} < 12$ . The same pattern holds true at other values of transverse momentum and pseudo-rapidity relevant for Hera energies and we find that both  $M$  and  $\mu$  slightly increase with the transverse momentum and the rapidity although the precise value of the scale is not important in the neighborhood of the optimal point. The features of scale compensation in perturbative calculations have been extensively studied since the pioneering works of Stevenson and Politzer [28]. In the case of reactions involving real photons the inhomogeneous term in eq. (4) introduces an added complication [26] which has led to some confusion in recent studies [4], [27]. When calculating the higher order corrections to the direct sub-processes ( $\gamma q \rightarrow g q$ ,  $\gamma g \rightarrow q \bar{q}$ ) and requiring one of the final partons to be at large  $p_T$  one has to integrate over a kinematical configuration where the photon decays, for exemple, into a real anti-quark and a virtual quark which can be on-shell. This leads to a divergence at the pole of the quark propagator (collinear configuration). The factorization scale separates the region of high quark virtuality which contributes to the higher order  $K_{i\gamma}^D$  term in eq. (2) and the region of small virtuality which is associated to the photon structure function and therefore to  $\frac{d\sigma^{SF}}{d\vec{p}_T d\eta}$ . Before QCD is turned on ( $\alpha_s = 0$ ) in the evolution equations (4), the cross section eq. (1) is exactly independent of the scale  $M$  which is just an arbitrary parameter which separates the hard regime from the soft (structure function) one. When QCD is turned on, the  $\ln M$  dependence is resummed to all orders in the structure function while the balancing term in  $K_{i\gamma}^D$  is not, thereby leading to a residual  $M$  dependence in the combination  $\frac{d\sigma^D}{d\vec{p}_T d\eta} + \frac{d\sigma^{SF}}{d\vec{p}_T d\eta}$  as is expected when working with a truncated perturbative series: the scale dependence is partially compensated between the higher order term of eq. (2) and the leading one in eq. (3) (variation associated to the inhomogeneous term,  $k_i$ , in eq. (4)) on the one hand, and between the two terms on the right hand side of eq. (3) (homogeneous term in eq. (4)). In no case, it is expected that  $\frac{d\sigma^D}{d\vec{p}_T d\eta}$  and  $\frac{d\sigma^{SF}}{d\vec{p}_T d\eta}$  be separately stable under changes of  $M$  and therefore they cannot be physical quantities to be compared with experiment. An apparent stability may however be obtained for  $\frac{d\sigma^{SF}}{d\vec{p}_T d\eta}$  when choosing  $M = \mu$ , so that the variation of the coupling partially cancels that of the photon structure

function.

To further test the practical effect of optimization we show in fig. 2) the rapidity distribution at fixed  $p_T = 8 \text{ GeV}/c$  under two hypotheses: the solid line shows the optimal result while the dashed line shows the predictions based on the commonly used choice  $M = \mu = p_T$ . The variation does not exceeds 8% with a moderate rapidity dependence: the optimization decreases slightly the predictions in the backward region (*i.e.* the photon fragmentation region) and increases them in the forward one. In the following, we keep the traditional choice  $M = \mu = p_T$  which turns out to be quite sufficient for comparison with present data. Also shown in the figure is the contribution of the direct term, eq. (2): it is negligible except in the backward region where it reaches 20% of the full cross section. Needless to recall that this result is only qualitative as the magnitude of the direct term varies much more than the full cross section under changes of scales.

We show in fig. 3a) the results of our calculation under the H1 experimental conditions. The rapidity distribution is obtained integrating over  $p_T > 7 \text{ GeV}/c$  and compared with the data [1]. The rising rapidity spectrum observed experimentally cannot be reproduced. Part of the problem at large  $\eta$  may be due to the contamination of the jet with particles from the "underlying" event which may play an important role given the rather low jet  $p_T$  values involved. In order to test the sensitivity of our predictions to structure functions we play the following extreme games: setting the gluon density in the photon to 0 gives the dashed curve with a totally wrong rapidity dependence while setting the gluon in the proton to 0 essentially decreases the cross section without changing the shape of the curve in the experimentally accessible domain. We also show the predictions assuming a vanishing  $VDM$  input: as expected only the forward rapidity domain is strongly affected. The only virtue of these games is to indicate which regions are important to constrain the various structure functions and what precision the data should reach to give quantitative constraints.

In the same spirit we plot in fig. 3b) the average momentum of the partons in the proton,  $\langle x_p \rangle$ , and in the electron,  $\langle x_e \rangle$ , as functions of the rapidity, for the cross section shown in fig. 3a). We note the small value of  $\langle x_p \rangle$  over the whole range confirming the important role played by the gluon in the proton as just seen above. When Hera data become precise enough they can effectively be used to constrain the proton structure function in the vicinity of  $x_p \simeq .05$  at values of  $Q^2$  around 50 to 100  $\text{GeV}^2$ . The average

value  $\langle x_e \rangle$  of the partons in the electron is obtained by convoluting the photon spectrum eq. (15) with the parton distribution in the photon and it is calculated here using only the  $SF$  component. The rather "large"  $\langle x_e \rangle$  obtained is due to the fact that the parton distributions in the photon are not as peaked as that in the proton. In the range considered by H1 the cross section is mostly sensitive to the quark density which is also probed in studies of  $F_2^\gamma$ . To achieve good sensitivity to the gluon distribution would require a larger rapidity coverage in the forward region.

In fig. 4), we plot the jet distribution in  $p_T$  after integration over the rapidity domain  $-1. < \eta < 1.5$ . Excellent agreement is reached both in magnitude and in shape. In view of fig. 3a) however it is clear that this agreement is purely fortuitous! This illustrates the fact that rapidity distributions are more powerful than transverse momentum ones to constrain the parameters of the theory.

In conclusion, we find the study of jet photoproduction at Hera very promising. Concerning the quantitative comparison between theory and experiment it appears that the relatively low values of the jet transverse momentum do not allow us to exclude the possibility of contamination of the jets with low  $p_T$  fragments of the proton making the extraction of the parton momentum from the jet momentum very difficult and the comparison with the theory rather dubious at this point of the analysis. This shows also the relevance of collecting data on inclusive particle production [3] at large transverse momentum which do not suffer from such an ambiguity. The extra degrees of freedom contained in the fragmentation functions are by now rather well constrained [29] and the comparison with theoretical calculations [30] on particle production would also be very useful to determine the parton distributions in the photon.

### **Acknowledgements**

We thank M. Erdmann for several enlightning discussions. We are indebted to the EEC programme "Human Capital and Mobility", Network "Physics at High Energy Colliders", contract CHRX-CT93-0357 (DG 12 COMA) for financial support.

## References

- [1] H1 collaboration, I. Abt et al., Phys. Lett. **B314** (1993) 436.
- [2] ZEUS collaboration, M. Derrick et al., Phys. Lett. **322** (1994) 287.
- [3] H1 collaboration, see also I. Abt et al., Phys. Lett. **B328** (1994) 176.
- [4] L.E. Gordon and J.K. Storrow, Phys. Lett. **B291** (1992) 320.
- [5] D. Bödeker, G. Kramer and S.G. Salesch, preprint DESY 94-042, March 1994.
- [6] The higher order corrections to the direct term have also been calculated by D. Bödeker Phys. Lett. **B192** (1992) 164, Z. Phys. **C59** (1993) 501, while those to the SF term are discussed by G. Kramer and S.G. Salesch, Z. Phys. **C61** (1994) 277 and M. Greco and A. Vicini, Nucl. Phys. **B415** (1994) 386.
- [7] F. Aversa, P. Chiappetta, M. Greco and J.Ph. Guillet, Nucl. Phys. **B327** (1989) 105; Z. Phys. **C46** (1990) 401; Phys. Rev. Lett. **65** (1990) 401.
- [8] P. Aurenche, J.-Ph. Guillet, M. Fontannaz, Y. Shimizu, J. Fujimoto and K. Kato, Prog. Theor. Phys. **92** (1994) 175.
- [9] P. Aurenche, P. Chiappetta, M. Fontannaz, J.Ph. Guillet and E. Pilon, Z. Phys. **C56** (1992) 589.
- [10] G. Curci, W. Furmanski and R. Petronzio, Nucl. Phys. **B175** (1980) 27.
- [11] R.K. Ellis, H. Georgi, M. Machacek, H.D. Politzer and G.C. Ross, Nucl. Phys. **B152** (1979) 285.
- [12] W. Furmanski and R. Petronzio, Phys. Lett. **B97** (1980) 435.
- [13] M. Fontannaz and E. Pilon, Phys. Rev. **D45** (1992) 382.
- [14] M. Glück, E. Reya and A. Vogt, Phys. Rev. **D45** (1992) 3986.
- [15] W.A. Bardeen, A.J. Buras, D.W. Duke and T. Muta, Phys. Rev. **D18** (1978) 3998.

- [16] M. Fontannaz, Orsay preprint LPTHE-93-22, talk given at the 21st International meeting on Fundamental Physics, Miraflores de la Sierra, Spain, May 1993;  
P. Aurenche, M. Fontannaz and J.Ph. Guillet, LPTHE 93-37, October 1993.
- [17] JADE collaboration, W. Bartel et al., Z. Phys. **C24** (1984) 231.
- [18] TASSO collaboration, M. Althoff et al., Z. Phys. **C31** (1986) 527.
- [19] PLUTO collaboration, Ch. Berger et al., Nucl. Phys. **B281** (1987) 365.
- [20] AMY collaboration, T. Sasaki et al., Phys. Lett. **B252** (1990) 491.
- [21] TOPAZ collaboration, H. Hayashii et al., Phys. Lett. **B314** (1993) 149.
- [22] P. Aurenche, R. Baier, M. Fontannaz, M.N. Kienzle-Focacci and M. Werlen, Phys. Lett. **B233** (1989) 517.
- [23] G.A. Schuler, CERN-TH.6427/92, proceedings of the DESY workshop on physics at HERA, Hamburg, Oct. 1991;  
F.M. Borzumati and G.A. Schuler, Z. Phys. **C58** (1993) 139.
- [24] P. Aurenche, J.-Ph. Guillet, M. Fontannaz, Y. Shimizu, J. Fujimoto and K. Kato, ENSLAPP-A-482/94 preprint, presented at the Workshop on two photon physics at LEP and HERA, Lund, May 1994.
- [25] P. Aurenche, R. Baier, M. Fontannaz, J. Owens and M. Werlen, Phys. Rev. **D39** (1989) 3275.
- [26] P. Aurenche, R. Baier, M. Fontannaz and D. Schiff, Nucl. Phys. **B286** (1987) 509; 553.
- [27] G. Kramer and S.G. Salesch, see [6].
- [28] P.M.Stevenson, Phys. Rev. **D23** (1981) 2916;  
P.M.Stevenson and R.Politzer, Nucl. Phys. **B277** (1986) 758.
- [29] P. Chiappetta, M. Greco, J.Ph. Guillet, S. Rolli and M. Werlen, Nucl. Phys. **B412** (1994) 3.

- [30] F.M. Borzumati, B.A. Kniehl and G. Kramer, Z. Phys. **C59** (1993) 341;  
B.A. Kniehl and G. Kramer. DESY 94-009;  
L.E. Gordon, Dortmund preprint DO-TH 93/25;  
P. Aurenche , M. Fontannaz, M. Greco and J.Ph. Guillet, in preparation.

## Figure Captions

- Fig. 1 Variation of the cross section at fixed  $p_T = 8 \text{ GeV}/c$  and  $\eta = 0$  as a function of the factorization scale  $M$  and the renormalization scale  $\mu$ : a) leading logarithmic approximation; b) next-to-leading logarithmic approximation; c) contour plot for the NTL approximation. The equal cross section lines are labeled in  $pb \text{ (GeV}/c)^{-1}$ .
- Fig. 2 Rapidity dependence of the cross section at fixed  $p_T = 8 \text{ GeV}/c$ : the solid curve is the optimized prediction while the dashed curve is obtained with the choice  $M = \mu = p_T$ . The dotted curve is the contribution of the direct term (multiplied by a factor 4).
- Fig. 3 a) Rapidity dependence of the theoretical predictions compared to the experimental data of H1. The dashed curve is obtained when  $F_{g/\gamma} = 0$  and the dotted one when  $F_{g/p} = 0$ . The dash-dotted curve results from the choice  $F_{i/\gamma}^{VDM} = 0$  in eq. (13).  
b) Average values of the scaled longitudinal momenta in the proton and the electron.
- Fig. 4 Transverse momentum dependence of the cross section integrated over the pseudo-rapidity range  $-1. < \eta < 1.5$  and comparison with H1 data.

This figure "fig1-1.png" is available in "png" format from:

<http://arxiv.org/ps/hep-ph/9409296v1>



$d\sigma/dP_t d\eta|_{\eta=0}$  (pb (GeV/c) $^{-1}$ )

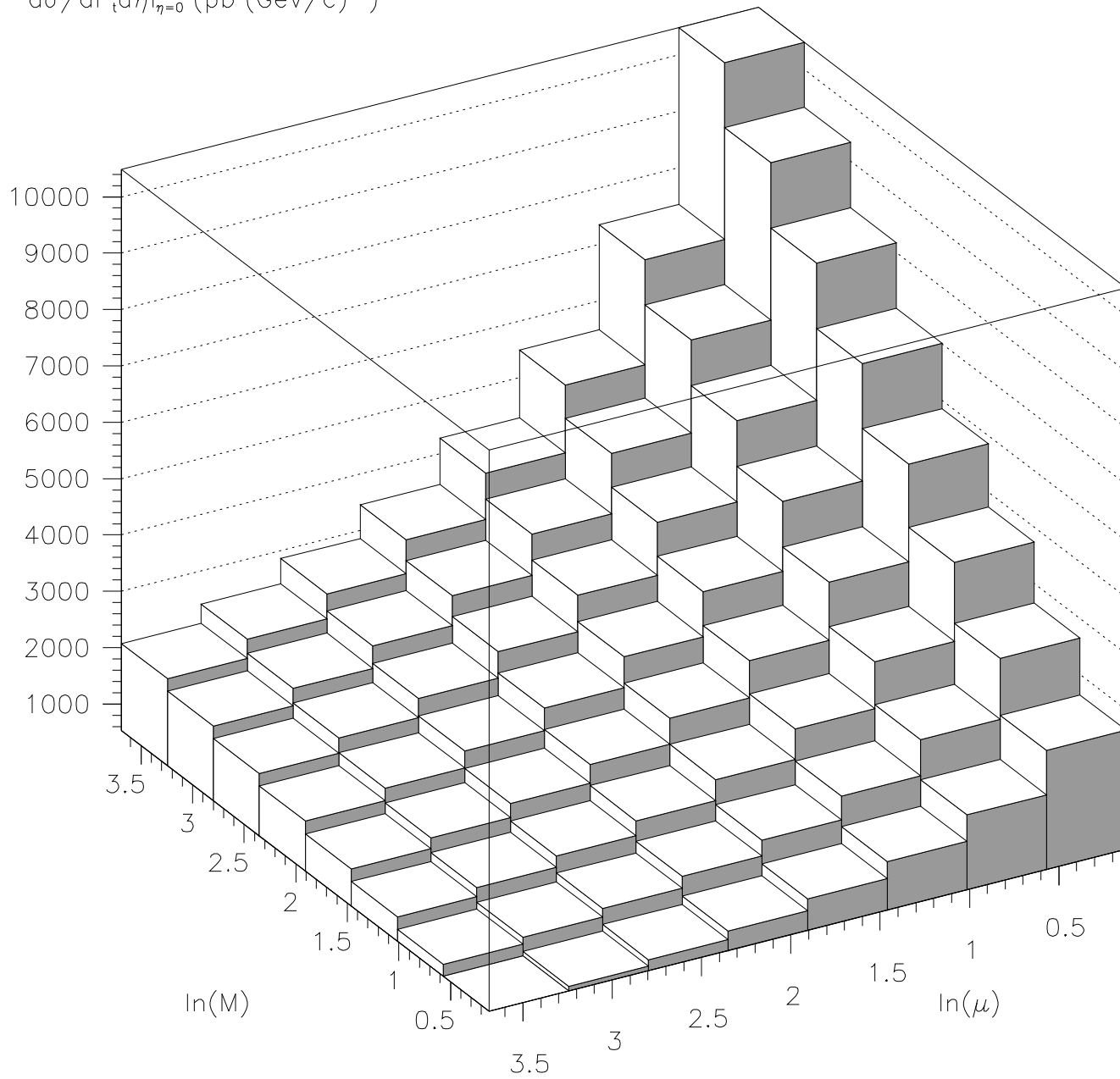


Fig. 1a

$$d\sigma/dP_t d\eta|_{\eta=0} \text{ (pb (GeV/c)}^{-1}\text{)}$$

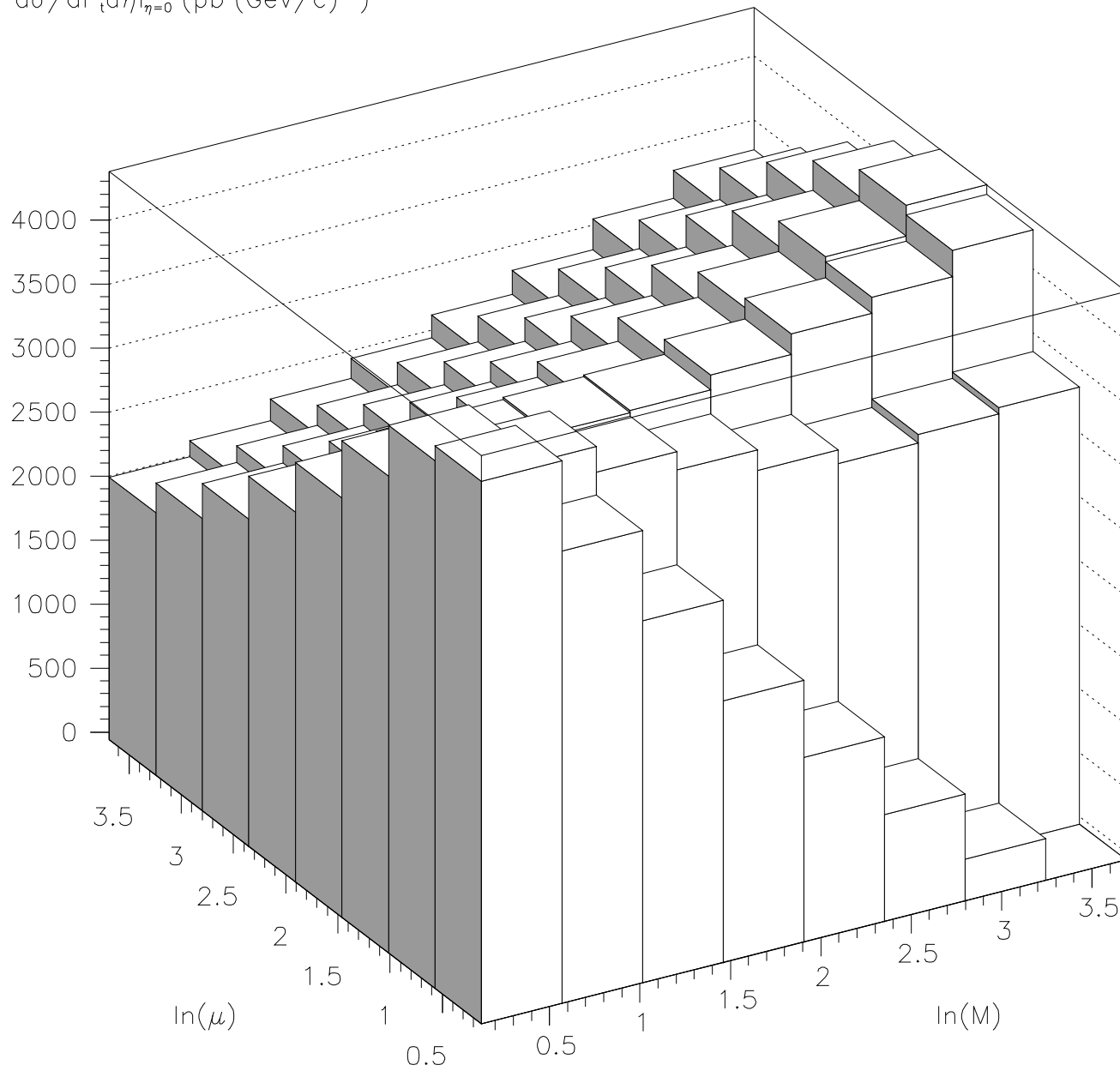


Fig. 1b

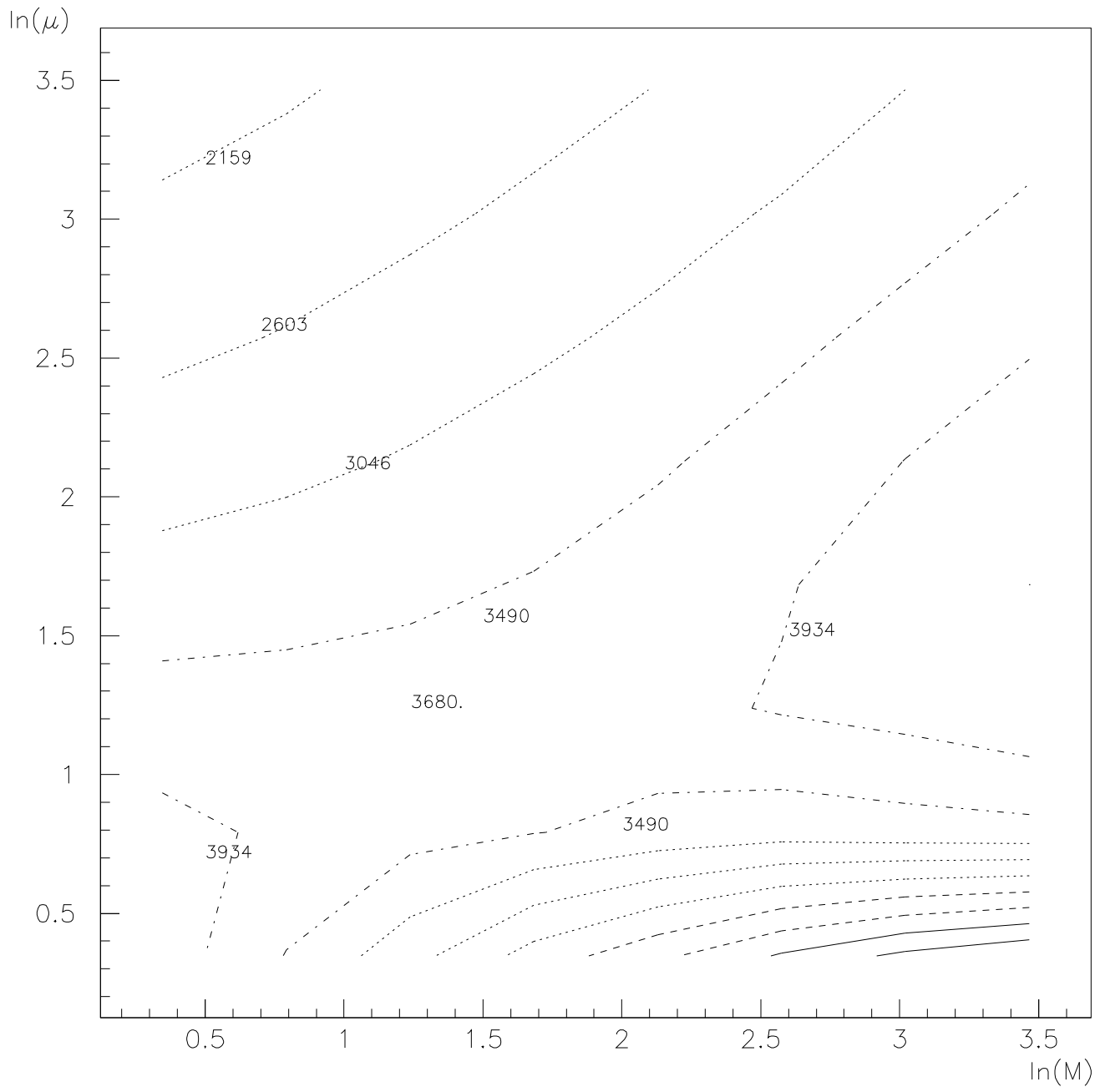


Fig. 1c

This figure "fig2-1.png" is available in "png" format from:

<http://arxiv.org/ps/hep-ph/9409296v1>

This figure "fig3-1.png" is available in "png" format from:

<http://arxiv.org/ps/hep-ph/9409296v1>

This figure "fig4-1.png" is available in "png" format from:

<http://arxiv.org/ps/hep-ph/9409296v1>

This figure "fig1-2.png" is available in "png" format from:

<http://arxiv.org/ps/hep-ph/9409296v1>

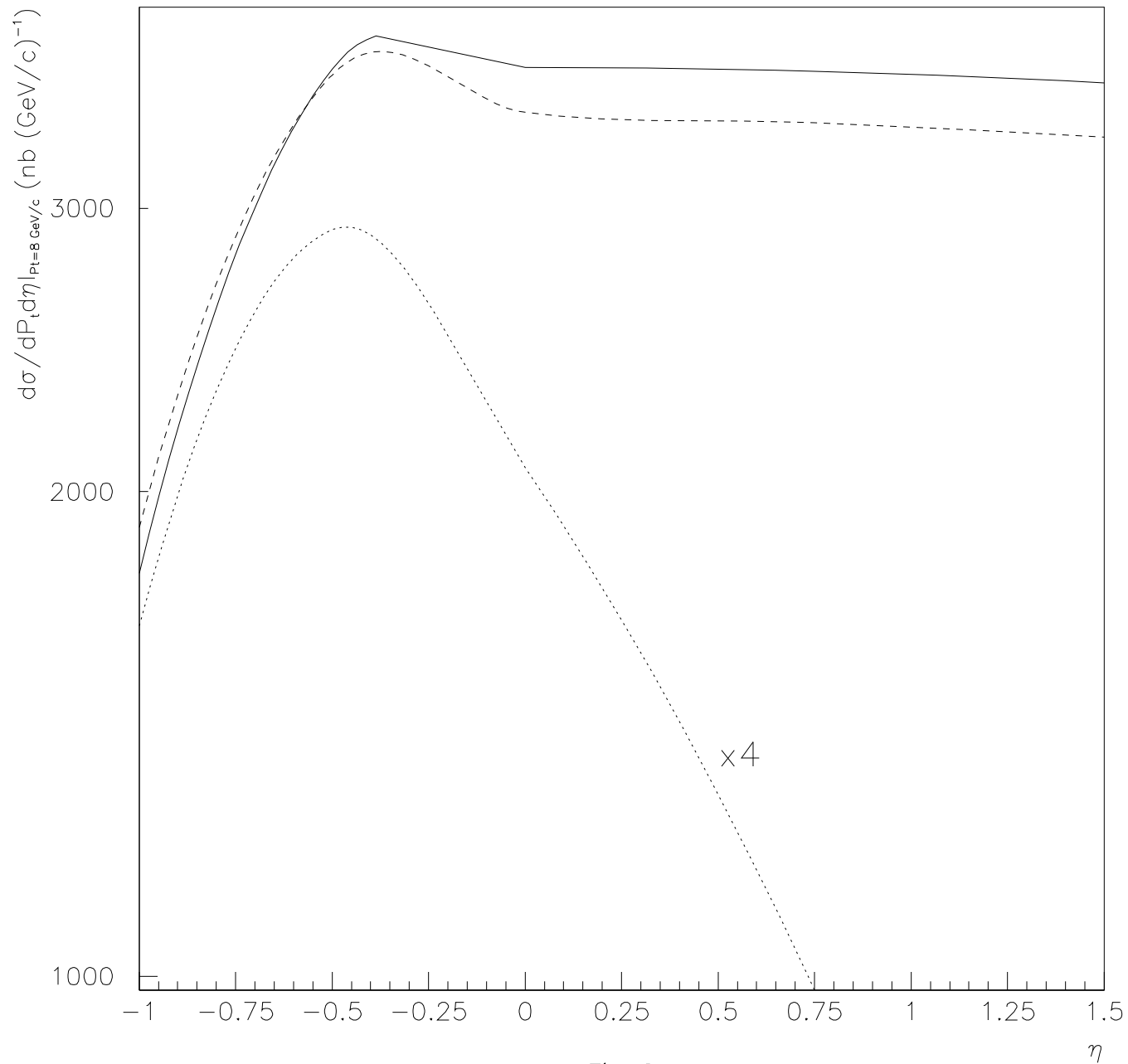


Fig. 2



This figure "fig3-2.png" is available in "png" format from:

<http://arxiv.org/ps/hep-ph/9409296v1>

This figure "fig1-3.png" is available in "png" format from:

<http://arxiv.org/ps/hep-ph/9409296v1>

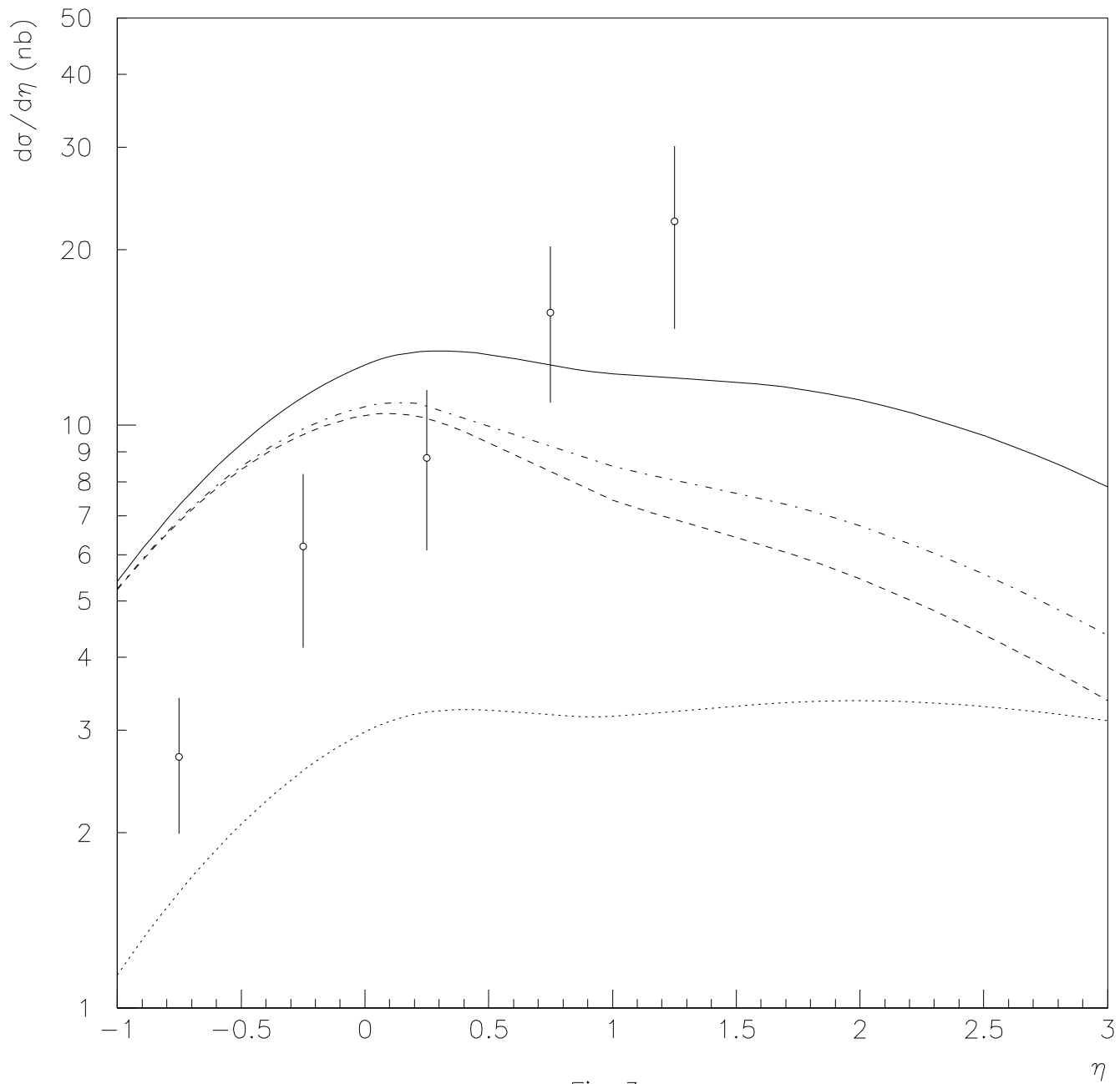


Fig. 3a

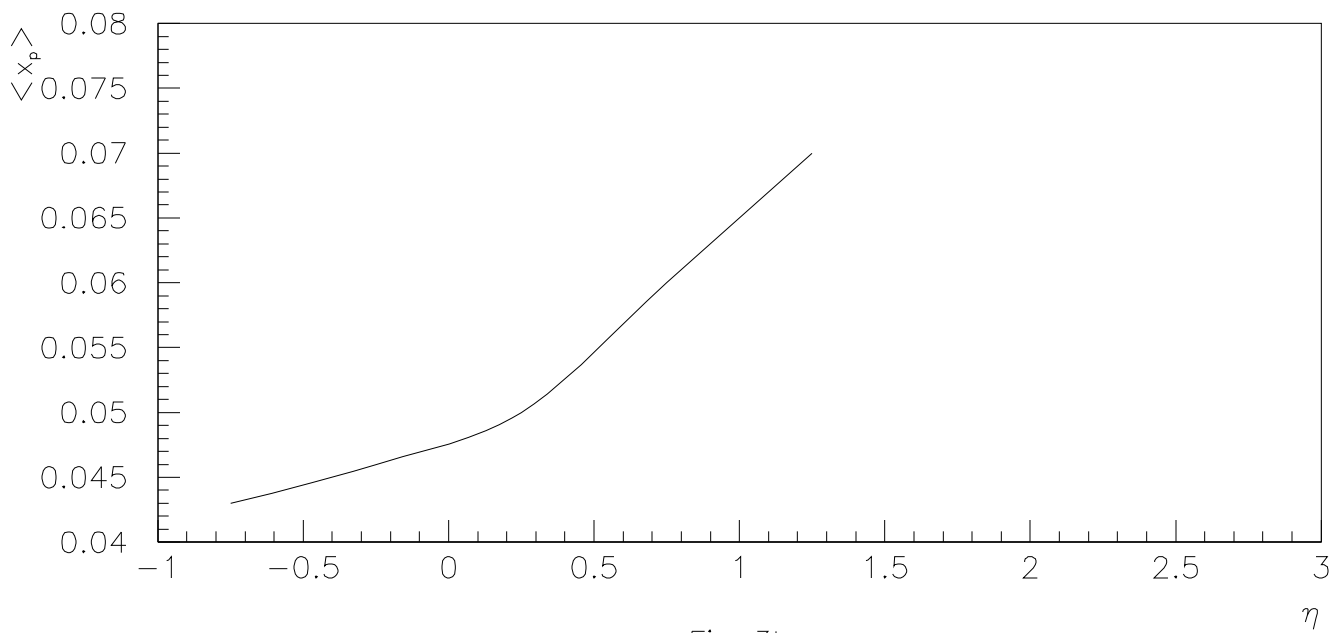
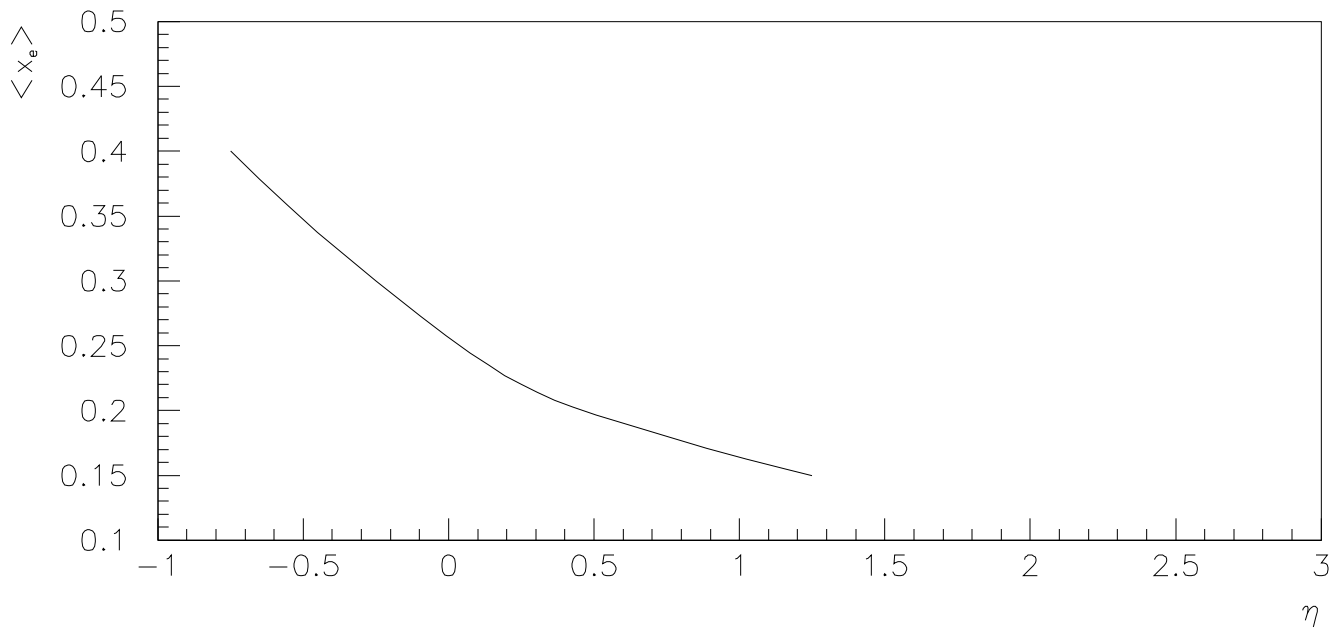


Fig. 3b

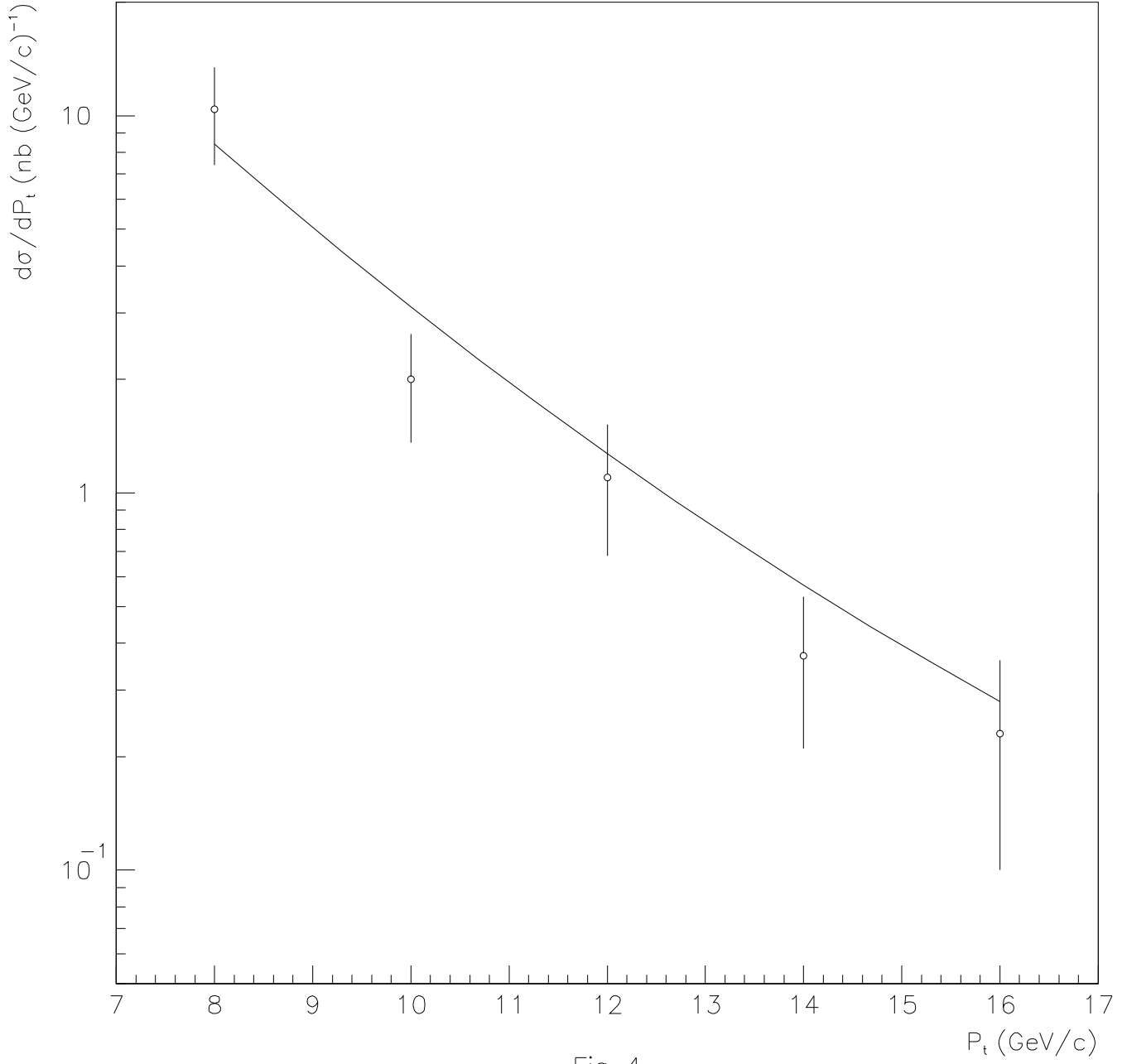


Fig. 4